A Numerical Study of Capsizing: Comparing Control Set Analysis and Melnikov's Method

January 11, 2006

Fritz Colonius[1], Edwin Kreuzer[2], Albert Marquardt[1], Wolfgang Sichermann[2]

[1]Institut für Mathematik
Universität Augsburg
86135 Augsburg, Germany

[2]Institut für Mechanik und Meerestechnik
Technische Universität Hamburg-Harburg
21071 Hamburg, Germany

Abstract: Two models for ship roll motion and capsizing under stochastic excitation are analyzed using Melnikov's method and control set analysis. The predictions given by these two methods are compared.

1 Introduction

A classical method to detect chaotic transitions in perturbed Hamiltonian systems is Melnikov's method (Guckenheimer and Holmes [9]; Wiggins [15]). Though designed as a tool for analyzing chaotic motions, it is also used to derive a (conservative) criterion for the loss of system integrity under deterministic or stochastic perturbations (Simiu [12]). Another approach to the investigation of system integrity with respect to deterministic or stochastic time-varying perturbations is the analysis of invariance and controllability properties of an associated control system and the support theorem of Stroock and Varadhan (Colonius, de la Rubia, and Kliemann [2]).

In the present paper, we compare these two methods by studying two simple models (in dimensionless form) describing ship roll motion under the action of ocean waves. In this special situation, we are able to give a thorough analysis using each of these methods. We show to which degree Melnikov's method gives conservative results. In particular, it turns out that for weakly perturbed Hamiltonian systems Melnikov's method accurately predicts when a controlled homoclinic or heteroclinic connection exists (here

the time-dependent excitation is substituted by piecewise constant control functions). We show that – under increasing amplitudes of the ocean waves – this always precedes the loss of invariance. The latter can be characterized by a control set analysis for which numerical tools are available.

The first model (Kreuzer and Sichermann [10]) has an $M-$shaped potential $V(x) = \frac{1}{2}x^2 - \frac{1}{4}\alpha x^4$ and a nonlinear viscous damping. For additive as well as multiplicative excitation the system is given by

$$\ddot{x} + \beta_1 \dot{x} + \beta_3 \dot{x}^3 + [1 + u_m(t)]x - \alpha x^3 = u_a(t); \tag{1}$$

here α, β_1, and β_3 are nonnegative parameters. The deterministic or random perturbations $u_m(t), u_a(t)$ take values in $[-\rho_m, \rho_m]$ and $[-\rho_a, \rho_a]$, respectively (see below for more specific descriptions).

The second system is the so-called escape equation with time-periodic excitation (see e.g. Soliman and Thompson [13], Nusse, Ott, and Yorke [11], Szolnoki [14], Gayer [8]). Here the potential is $V(x) = \frac{1}{2}x^2 - \frac{1}{3}x^3$ with linear viscous damping under the influence of a periodic driving force,

$$\ddot{x} + \gamma\, \dot{x} + x - x^2 = F\, \sin \omega t + u_a(t) \tag{2}$$

with nonnegative parameters γ, ω, and F. Again the deterministic or random perturbations $u_a(t)$ take values in $[-\rho_a, \rho_a]$. In this system we only consider additive perturbations. Note, however, that we allow for a dominant periodic component in the perturbations, while the perturbations in the first system are unstructured. For both systems we will consider the question if capsizing occurs, i.e., if the system leaves the potential well with positive probability. Here we will analyze the behavior for varying maximal amplitudes ρ_a and ρ_m of the perturbations.

We note that the two methods are not directly comparable, since control set analysis gives results for fixed parameters, while Melnikov's method only claims results for sufficiently small $\varepsilon-$perturbations from (Hamiltonian) systems with homo- or heteroclinic orbits. Hence we will also perform control set analysis for varying ε.

The paper is organized as follows: In Section 2, we present some essential facts on the relation between the stochastic systems and associated control systems. Section 3 provides a controllability analysis for the system with $M-$potential, while in Section 4 Melnikov's method is applied and the results are compared. Section 5 presents an analogous discussion for the escape equation. Final Section 6 summarizes our major findings and conclusions.

2 Background on Control Set Analysis

In this section we recall some facts from [2], [3] about Markov diffusion systems and their relations to associated control systems. In order to avoid undue technicalities, we mainly discuss the ship roll model (1); modifications necessary for the periodically excited system (2) are indicated at the end of the section.

We start with a slightly more general version of system (1) with stochastic perturbations in the form

$$\ddot{x} + \beta_1 \dot{x} + \beta_3 \dot{x}^3 + [1 + \sum_{i=1}^{N} \gamma_i \cos \eta_i(t)]x - \alpha x^3 = \sum_{i=N+1}^{M} \gamma_i \cos \eta_i(t), \qquad (3)$$

where $\gamma_i > 0$ and the background noise $\eta = (\eta_i)$ is determined by

$$\mathrm{d}\eta_i = \Omega_i t + D_i \mathrm{d}W_i \text{ for } i = 0, 1, ..., M,$$

with independent white noise $\mathrm{d}W_i$ with intensity $D_i > 0$.

Writing this, as usual, as a first order equation one obtains the planar system

$$\dot{x}_1 = x_2,\ \dot{x}_2 = -\beta_1 x_2 - \beta_3 x_2^3 - x_1 + \alpha x_1^3 - x_1 \sum_{i=1}^{N} \gamma_i \cos \eta_i + \sum_{i=N+1}^{M} \gamma_i \cos \eta_i.$$

The corresponding control system is

$$\dot{x}_1 = x_2,\ \dot{x}_2 = -\beta_1 x_2 - \beta_3 x_2^3 - x_1 + \alpha x_1^3 - x_1 \sum_{i=1}^{N} \gamma_i u_i(t) + \sum_{i=N+1}^{M} \gamma_i u_i(t);$$

here, formally, $\cos \eta_i$ has been replaced by arbitrary piecewise continuous functions $u_i(t)$ taking values in $[-1, 1]$; the u_i are considered as controls.

Remark 2.1 *We remark that, alternatively, the same noise may act additively and multiplicatively. This is easily taken into account by inserting the same control function in the additive and multiplicative terms.*

Obviously, the controllability properties of this system are the same as those of the system with only two controls

$$\dot{x}_1 = x_2,\ \dot{x}_2 = -\beta_1 x_2 - \beta_3 x_2^3 - x_1 + \alpha x_1^3 - u_m(t) x_1 + u_a(t), \qquad (4)$$

where

$$(u_m(t), u_a(t)) \in [-\rho_m, \rho_m] \times [-\rho_a, \rho_a] \text{ and } \rho_m := \sum_{i=1}^{N} \gamma_i \text{ and } \rho_a := \sum_{i=N+1}^{M} \gamma_i.$$

In other words: the controllability properties of the corresponding deterministic system are independent of the number of the stochastic perturbations. Hence we restrict attention to just one additive perturbation η_a and one multiplicative perturbation η_m. Then the stochastic system (3) (with $N = 1, M = 2$) corresponding to (4) may be considered with state variables (x, η_a, η_m) in the state space $\mathbb{R}^2 \times \mathbb{S}^1 \times \mathbb{S}^1$, where $\mathbb{S}^1$ denotes the unit circle parametrized by $[0, 2\pi)$.

We need some notations and results from control theory (see [5] for a thorough discussion). Denote the solution of (4) with initial state $x \in \mathbb{R}^2$ at time $t = 0$ by $\varphi(t, x, u)$. It depends on the control function $u = (u_a, u_m)$ in the set $\mathcal{U}$ of control functions determined by the parameter $\rho = (\rho_a, \rho_m)$; dependence on ρ is here suppressed in the notation. The positive and negative orbits at time $t > 0$ are

$$\mathcal{O}_t^+(x) = \{\varphi(t, x, u),\ u \in \mathcal{U}\},\ \mathcal{O}_t^-(x) = \{\varphi(-t, x, u),\ u \in \mathcal{U}\},$$

and we set

$$\mathcal{O}_{\leq T}^+(x) = \bigcup_{t \in [0,T]} \mathcal{O}_t^+(x),\ \mathcal{O}_{\leq T}^-(x) = \bigcup_{t \in [0,T]} \mathcal{O}_t^-(x), \mathcal{O}^+(x) = \bigcup_{t \in [0,\infty)} \mathcal{O}_t^+(x).$$

A set $D \subset M$ with nonvoid interior is a control set if it is a maximal set with the property $D \subset \mathrm{cl}\mathcal{O}^+(x)$ for every $x \in D$. A control set D with $D = \mathrm{cl}\mathcal{O}^+(x)$ for every $x \in D$ is an invariant control set, the others are called variant. If $\rho_a > 0$, the considered system is locally accessible, i.e., for all $x \in \mathbb{R}^2$

$$\mathrm{int}\mathcal{O}_{\leq T}^+(x) \neq \varnothing \text{ and } \mathrm{int}\mathcal{O}_{\leq T}^-(x) \neq \varnothing \text{ for all } T > 0.$$

Then $\mathrm{int}D \subset \mathcal{O}^+(x)$ for all $x \in D$. If only multiplicative perturbations act on the system (i.e., $\rho_a = 0$), the origin in $\mathbb{R}^2$ remains fixed and local accessibility holds on $\mathbb{R}^2 \setminus \{0\}$.

Note that for system (3), (4) the required (Lie algebraic) assumptions from [2], [4], [3] are satisfied. The background noise η admits a unique invariant measure on $N = \mathbb{S}^1 \times \mathbb{S}^1$. The natural probability space to work

in is $\hat{\Omega} := \mathcal{C}(\mathbb{R}_0^+, \mathbb{R}^2 \times N) = \{\omega : R_0^+ \to \mathbb{R}^2 \times N, \text{ continuous}\}$ and for fixed initial conditions $(x, q) \in \mathbb{R}^2 \times N$ the pair process (4) induces a probability measure $\hat{P}_{(x,q)}$ on $\hat{\Omega}$. By $\hat{P}_{(x,\eta^*)}$ we denote the measure corresponding to the stationary Markov solution $\{\eta_t^*, t \geq 0\}$ in the $\eta-$component. Its marginal distribution on $\Omega := \mathcal{C}(\mathbb{R}_0^+, \mathbb{R}^2)$ will be denoted by $P_x, x \in \mathbb{R}^2$. The trajectories of the pair process are $(\varphi(t, (x, q), \omega), \eta(t, q, \omega))$ for $(x, q) \in \mathbb{R}^2 \times N$, and we will write the $x-$component under $\{\eta_t^*, t \geq 0\}$ as $\varphi(t, x, \omega)$, $x \in \mathbb{R}^2$. The transition probability from $x \in \mathbb{R}^2$ to a set $A \subset \mathbb{R}^2$ in time $t \geq 0$ is

$$P(t, x, A) = P_x(\varphi(t, x, \omega) \in A).$$

Using the tube method introduced by Arnold and Kliemann, it follows from the support theorem of Stroock and Varadhan that

$$\text{supp } P(t, x, \cdot) = \text{cl} \left\{ \begin{array}{c} y \in \mathbb{R}^2 \mid \text{ there is a piecewise continuous} \\ u \in \mathcal{U} \text{ such that } \varphi(t, x, u) = y \end{array} \right\}.$$

It now follows from [4] that the invariant Markov probability measures μ of (4) have support given by $\text{supp}\mu = D \times N$, where D is an invariant control set of (4), and these measures are unique on each set of this form. Every bounded invariant control set D of (4) has the property that $D \times N$ is the support of some invariant Markov measure. All other points in $\mathbb{R}^2 \times N$ are transient.

In order to describe the consequences of the support theorem for the relationship between the Markov diffusion process and the control system in more detail, we define the *first exit time* from a set $A \subset \mathbb{R}^2$ starting at a point $x \in \mathbb{R}^2$ as the random variable

$$\sigma_x(A) := \inf\{t \geq 0, \ \varphi(t, x, \omega) \notin A\}.$$

Due to Theorem 3.19 in [4], for invariant control sets $D \subset \mathbb{R}^2$ of system (4) the equation $P_x(\sigma_x(D) < \infty) = 0$ holds for all $x \in D$. For bounded variant control sets $D \subset \mathbb{R}^2$ on the other hand, it holds that $P_x(\sigma_x(D) < \infty) = 1$ for all $x \in D$. Under the measure P_x we even have that the expectation of the sojourn time $E_x[\sigma_x(D)]$ is finite. Furthermore, for an invariant control set D every point in the set

$$\{x \in \mathbb{R}^2, \text{ for all } u \in \mathcal{U} \text{ there is } T > 0 \text{ with } \varphi(T, x, u) \in D\}$$

has finite first entrance time into D with probability one.

In conclusion we see that the question if capsizing occurs in finite time in system (3) occurs with positive probability with the origin as initial value,

is equivalent to existence an invariant control set (around the origin). If only multiplicative perturbations act, the origin is invariant, and one has to look for initial values near the origin. For computation of the capsizing probabilities, we have to recur to Monte Carlo simulation (see e.g. [3]).

For the periodic escape equation (2), similar concepts can be applied by adding $t \in [0, 2\pi)$ to the state variables (see Gayer [8]). It is well known that the behavior of the differential equation

$$\ddot{x} + \gamma\,\dot{x} + x - x^2 = 0$$

may change drastically, when time-periodic perturbations act. For example, bifurcations may occur with respect to $F \geq 0$ in

$$\ddot{x} + \gamma\,\dot{x} + x - x^2 = F\,\sin\omega t.$$

If the intensity D_i of the noise η_i is very small it is not adequate to insert an arbitrary control. Instead it will be more appropriate to consider stochastic perturbations of this periodic differential equation as in Section 5.

3 Control Set Analysis for the M–Potential

In this section we give a description of the controllability properties of system (3) in the phase plane and discuss the consequences for the stochastically perturbed system.

We first consider the deterministic control system (4) and throughout we restrict the analysis to the technically relevant parameter values (for following seas) given in Kreuzer and Sichermann [10]

$$\alpha = 0.674,\ \beta_1 = 0.231,\ \beta_3 = 0.375.$$

A sketch of the corresponding M–potential

$$V(x) = \frac{1}{2}x^2 - \frac{\alpha}{4}x^4, \quad \frac{\partial V(x)}{\partial x} = x - \alpha x^3$$

is shown in Figure 1. It is easily seen that the unperturbed system (i.e., $u_a = u_m = 0$) has three equilibria, the asymptotically stable equilibrium $e_0 = 0$ at the origin and hyperbolic equilibria e_1 and e_2 on the negative and positive x_1-axis, respectively. Without damping, we obtain a Hamiltonian system with two heteroclinic orbits connecting the hyperbolic equilibria (Figure 1).

For small ρ_a, ρ_m there are an invariant control set $D_0(\rho_a, \rho_m)$ around the origin and two variant control sets $D_1(\rho_a, \rho_m)$ and $D_2(\rho_a, \rho_m)$ around

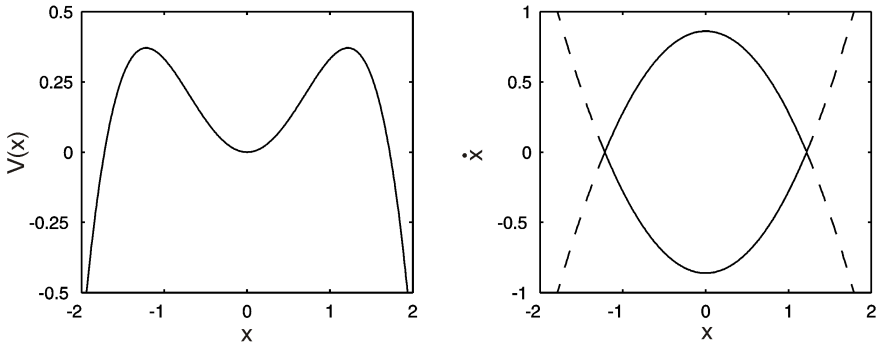

Figure 1: M–potential (left) and heteroclinic orbits of the associated Hamiltonian system (right).

the hyperbolic equilibria (for $(\rho_a, \rho_m) \to (0,0)$ they converge to the corresponding equilibria). Numerical experiments indicate that in addition to this regime, there are two further regimes, depending on $\rho = (\rho_a, \rho_m)$. For increasing $\rho-$values, the two control sets around the hyperbolic equilibria are first connected by 'control heteroclinic' trajectories and merge and form a control set $D_{12}(\rho)$. Only later they merge with the invariant control set and form a control set $D_{012}(\rho)$ containing the origin; here invariance is lost. Typical situations are shown in Figures 2, 3, 4 and 5.

For a quantitative description we specify two curves in $\rho_a - \rho_m-$space, where these qualitative changes occur.

Definition 3.1 *The heteroclinic margin is*

$$H(\rho_a) = \inf\{\rho_m > 0,\ \exists D_{12}(\rho_a, \rho_m)\},$$

and the invariance margin is

$$I(\rho_a) = \inf\{\rho_m > 0,\ \exists D_{012}(\rho_a, \rho_m)\}.$$

The results in the preceding section imply that as long as the invariant control set $D_0(\rho)$ exists, the system remains with probability one in the potential well, more precisely, in the set $\{x \in \mathbb{R}^2,$ for all $u \in \mathcal{U}$ there is $T > 0$ with $\varphi(T, x, u) \in D_0\}$. Outside of this set, the ship will capsize with probability one. If the invariant control set has vanished (i.e., $\rho_m > I(\rho_a)$), the ship will capsize from any initial point with probability one. It is clear that for applications the invariance margin is the relevant object. On the

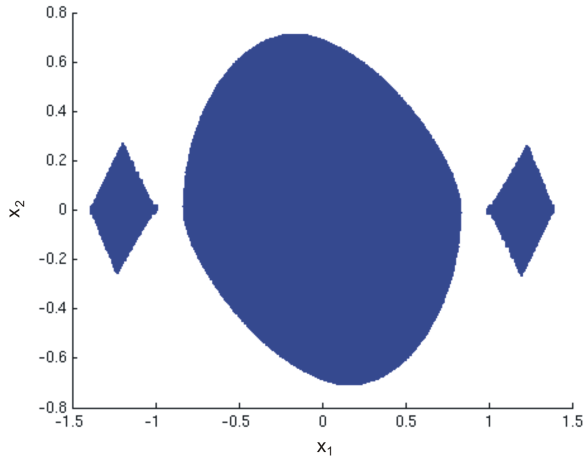

Figure 2: The regime for small amplitudes: one invariant control set D_0 in the center, two variant control sets D_1 (on the left) and D_2 (on the right) around the hyperbolic equilibria ($\rho_a = 0.20, \rho_m = 0.10$).

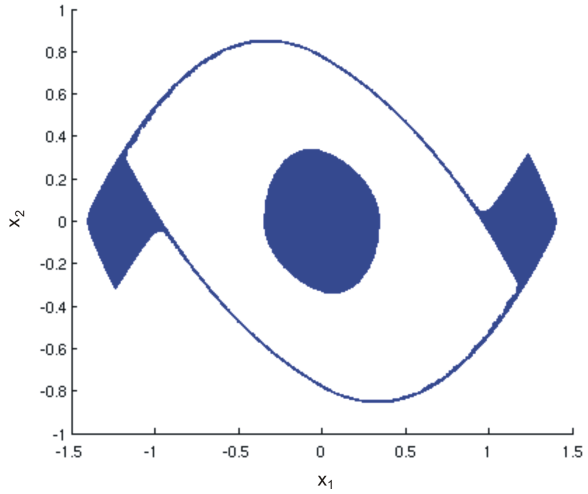

Figure 3: Heteroclinic regime: one invariant control set D_0 in the center, one variant control set D_{12} containing both hyperbolic equilibria ($\rho_a = 0.00, \rho_m = 0.37$).

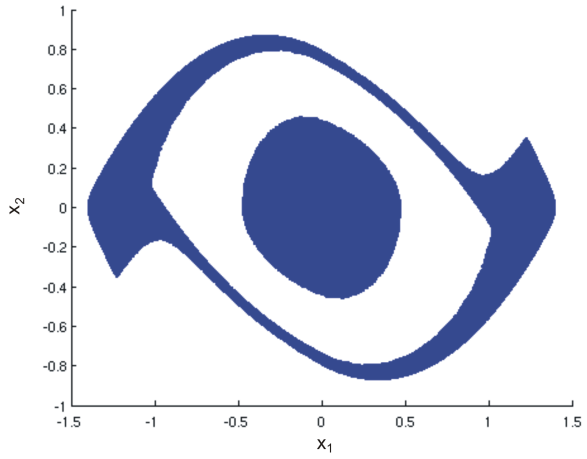

Figure 4: Heteroclinic regime: one invariant control set D_0 in the center, one variant control set D_{12} containing both hyperbolic equilibria ($\rho_a = 0.00, \rho_m = 0.40$).

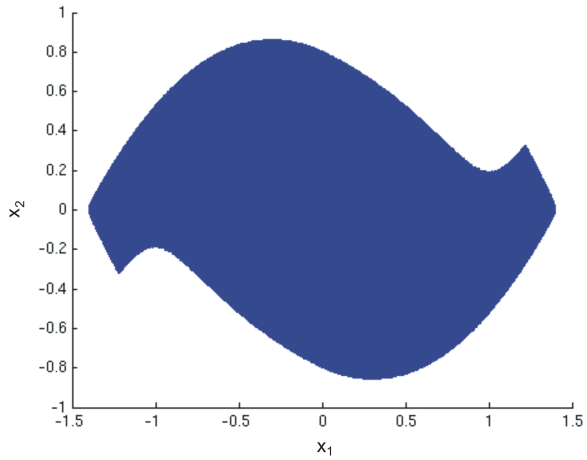

Figure 5: Variant regime: only one control set D_{012} which is variant ($\rho_a = 0.30, \rho_m = 0.06$).

other hand, the heteroclinic margin is important in order to understand the mechanisms leading to loss of invariance.

The numerical computations of control sets are based on set-valued numerics (Dellnitz and Hohmann [6]); we use the MATLAB version of the program package GAIO from Junge. The control sets are found using the implementation due to Szolnoki [14]. If we fix the amplitude $\rho_a \geq 0$ of the additive perturbations, one can numerically determine the invariance margin by bisection. This yields the following results for the invariance margin $I(\rho_a)$

$$I(0) \in (0.42, 0.43)$$

and for $I^{-1}(\rho_m)$

$$\begin{aligned} &I^{-1}(0.0) \in (0.21, 0.22),\ I^{-1}(0.1) \in (0.15, 0.16), \\ &I^{-1}(0.2) \in (0.10, 0.11),\ I^{-1}(0.3) \in (0.05, 0.06). \end{aligned} \tag{5}$$

Thus we obtain an approximately linear relation given by

$$I(\rho_a) \approx -2\rho_a + 0.42. \tag{6}$$

Numerical computation of control sets near mergers is notoriously difficult. Hence we also follow an alternative approach to determine the heteroclinic and the invariance margin. It is based on numerical computation of stable and unstable manifolds, also performed using GAIO. This approach uses special properties of the considered second order system.

3.1 The Heteroclinic Margin

First we observe that the control system (3) is symmetric with respect to the x_2-axis in the following sense: For every solution $(x_1(t), x_2(t))$ one finds that $(y_1(t), y_2(t)) := (-x_1(t), -x_2(t))$ satisfies

$$\begin{aligned} \dot{y}_1 &= y_2 \\ \dot{y}_2 &= -\dot{x}_2 = \beta_1 x_2 + \beta_3 x_2^3 + x_1 - \alpha x_1^3 + u_m(t) x_1 - u_a(t) \\ &= -\beta_1 y_2 - \beta_3 y_2^3 - y_1 + \alpha y_1^3 - u_m(t) y_1 - u_a(t). \end{aligned}$$

Thus

$$\varphi(t, x_1, x_2, u_a, u_m) = -\varphi(t, -x_1, -x_2, -u_a, u_m).$$

This implies for every control set D that also $-D$ is a control set (here $D = -D$ is possible). Hence we restrict our analysis to the lower halfplane with $x_2 \leq 0$.

The equilibria of the system (3) with constant controls are given by $x_2 = 0$ and the three roots of

$$-x_1 + \alpha x_1^3 + u_a = 0.$$

There are three equilibria, all on the x_1-axis, one near the origin and denoted by $e_0(\rho_a)$ and two hyperbolic equilibria denoted by $e_1(\rho_a)$ and $e_2(\rho_a)$ (note that they are independent of ρ_m). For $u_a = 0$ the origin is an equilibrium and the hyperbolic equilibria $e_2(\rho_a = 0)$ and $e_1(\rho_a = 0)$ have abscissa given by

$$x_1 = \pm\sqrt{1/\alpha} = \pm\sqrt{1/0.674} \approx \pm 1.2181.$$

A phase plane analysis shows that, for given $\rho = (\rho_a, \rho_m)$, there are sets of complete controllability around the hyperbolic equilibria: For the set around the equilibrium $e_2(0)$, the left-most point on the x_1-axis is the hyperbolic equilibrium $e_2(\rho_a)$ corresponding to $u_a = \rho_a$ and the right-most point is the hyperbolic equilibrium $e_2(-\rho_a)$ corresponding to $u_a = -\rho_a$. Analogously, the set of complete controllability around $e_1(0)$ has as left-most point the equilibrium $e_1(\rho_a)$ and as right-most point the equilibrium $e_1(-\rho_a)$. For $\rho_m \leq H(\rho_a)$, these sets are control sets D_2 and D_1. If ρ_m is in the interval $(H(\rho_a), I(\rho_a)]$ they are both contained in a single control set D_{12}, but they are still maximal within a neighborhood, and hence called local control sets. The boundary of the (local) control set D_2 is given by parts of the unstable and stable manifolds of the equilibria $e_2(\rho_a)$ and $e_2(-\rho_a)$, analogously for D_1.

The trajectories obey the following monotonicity condition: Since

$$\dot{x}_2 = -\beta_1 x_2 - \beta_3 x_2^3 - x_1 + \alpha x_1^3 - u_m(t)x_1 + u_a(t),$$

one finds for constant controls and $t > 0$ that the second state component satisfies for $x_1 > 0$

$$u_m > u'_m \text{ and } u_a \leq u'_a \text{ implies } \varphi_2(t, x, u_m, u_a) < \varphi_2(t, x, u'_m, u'_a), \qquad (7)$$

and for $x_1 < 0$

$$u_m > u'_m \text{ and } u_a \geq u'_a \text{ implies } \varphi_2(t, x, u_m, u_a) > \varphi_2(t, x, u'_m, u'_a), \qquad (8)$$

Now consider the unstable manifolds $W^-(e_2(-\rho_a), \rho_m, -\rho_a)$ of the equilibrium $e_2(-\rho_a)$ and the stable manifold $W^+(e_1(-\rho_a), \rho_m, -\rho_a)$ of the equilibrium $e_1(-\rho_a)$. They intersect the negative x_2- axis transversally in unique points with ordinate

$$w^-(\rho_m, -\rho_a) \text{ and } w^+(-\rho_m, -\rho_a).$$

As a consequence of (7) and (8), one finds the following monotonicity properties (consider the unstable manifold in the quadrant $x_1 > 0, x_2 < 0$ and the stable manifold in the quadrant $x_1 < 0, x_2 < 0$):

$$\text{if } \rho_m > \rho'_m, \text{ then } w^-(\rho_m, -\rho_a) < w^-(\rho'_m, -\rho_a),$$
$$\text{if } \rho_m > \rho'_m, \text{ then } w^+(-\rho_m, -\rho_a) > w^+(-\rho'_m, -\rho_a).$$

This implies that for fixed ρ_a, there is a unique $\rho_m = \rho_m(\rho_a)$ with

$$w^-(\rho_m, -\rho_a) = w^+(-\rho_m, -\rho_a).$$

Furthermore, only for $\rho_m > \rho_m(\rho_a)$ it is possible to steer the system from D_2 to D_1. Using the symmetry property indicated above, it follows that one obtains a completely analogous situation in the upper halfplane. Thus we conclude that $H(\rho_a) = \rho_m(\rho_a)$ (see Figure 3 for an illustration of the control sets where $\rho_m - H(\rho_a) > 0$ is small). This reduces computation of the heteroclinic margin to computation of stable and unstable manifolds and their intersections with the x_2-axis. Thus, using bisection, one can approximate $H(\rho_a)$.

Figure 6 depicts the situation in the lower half plane. It shows part of the stable manifold (to the left of the x_2-axis) and the unstable manifold (to the right of the x_2-axis). On the left hand side are results for $\rho_m < H(\rho_a)$, i.e., the two control sets around the hyperbolic equilibria remain distinct, and on the right hand side are results for $\rho_m > H(\rho_a)$, i.e. the control set D_{12} containing the right and left equilibria exists. It turns out that numerically the heteroclinic margin is approximately linear. More precisely, we obtain the following results for $H(\rho_a)$

$$H(0.00) \in (0.37, 0.38),\ H(0.01) \in (0.35, 0.36),\ H(0.11) \in (0.180, 0.185),$$

and for $H^{-1}(\rho_m)$

$$H^{-1}(0.02) \in (0.20, 0.21),\ H^{-1}(0.00) \in (0.22, 0.23). \tag{9}$$

Note that Figure 3 shows a numerically computed set D_{12} which in fact, as indicated above, does not exist, since $H(0) > 0.37$.

These results were obtained using GAIO (computing times on a LINUX PC with 2.8 Mz approximately 90 minutes for standard box depth 26; where needed, box depth is taken as 28 with computing time approximately 150 minutes).

For a comparison of these results with Melnikov's method, it will also be necessary to consider the equations

$$\dot{x}_1 = x_2,\ \dot{x}_2 = -\varepsilon\beta_1 x_2 - \varepsilon\beta_3 x_2^3 - x_1 + \alpha x_1^3 - \varepsilon u_m(t) x_1 + \varepsilon u_a(t). \tag{10}$$

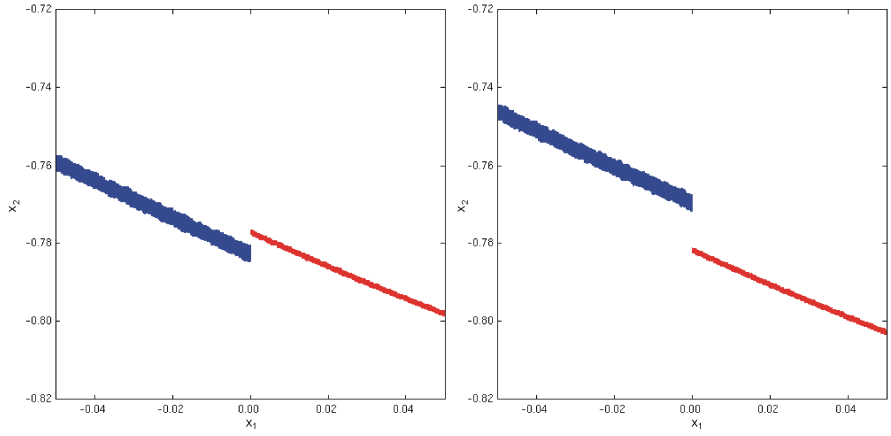

Figure 6: Stable manifolds $W^+(e_1(-\rho_a), -\rho_m, -\rho_a)$ and unstable manifolds $W^-(e_2(-\rho_a), \rho_m, -\rho_a)$ near the x_2-axis for $\rho_a = 0.000$ and $\rho_m = 0.370$ (left) and $\rho_m = 0.380$ (right).

They represent small perturbations from the Hamiltonian situation. One obtains

$$\text{for } \varepsilon = \frac{1}{2} : H(0) \in (0.385, 0.395),\ H^{-1}(0) \in (0.230, 0.240); \tag{11}$$
$$\text{for } \varepsilon = \frac{1}{4} : H(0) \in (0.390.0.400),\ H^{-1}(0) \in (0.235, 0.245).$$

3.2 The Invariance Margin

Next we turn to the computation of the invariance margin $I(\rho_a)$. First we show that

$$H(\rho_a) < I(\rho_a). \tag{12}$$

In fact, for $\rho_m = H(\rho_a)$ consider the trajectory $\hat{\varphi}$ starting in the left-most point $e_2(\rho_a)$ of the control set D_2 with control

$$u_a = -\rho_a \text{ and } \hat{u}_m = \begin{cases} \rho_m & \text{in the quadrant } x_1 > 0, x_2 \leq 0 \\ -\rho_m & \text{in the quadrant } x_1 \leq 0, x_2 \leq 0 \end{cases} . \tag{13}$$

This is the trajectory minimizing the x_2-component. It reaches the x_1-axis in finite time $t > 0$. In the quadrant $x_1 > 0, x_2 \leq 0$ it remains above the unstable manifold $W^-(e_2(-\rho_a), \rho_m, -\rho_a)$ and in the quadrant $x_1 \leq 0, x_2 \leq 0$

it remains above the stable manifold $W^+(e_1(-\rho_a), -\rho_m, -\rho_a)$. Thus, using monotonicity again, the region bounded by the x_2-axis and $\hat{\varphi}(t)$ in the lower half plane can only be left through the x_2-axis. Analogous properties hold in the upper halfplane. Thus there exists an invariant control set in this positively invariant region (cp. [5, Theorem 3.1.5]). The same situation occurs if $\rho_m > H(\rho_a)$ and the trajectory $\hat{\varphi}$ intersects (for the first time) the x_2-axis above the point $w^+(-\rho_m, -\rho_a)$, cp. Figure 7.

Note that the bounded region R bounded by the control set D_{12} is positively invariant; this follows from the definition of control sets as maximal sets of complete controllability and the fact that every point R can be reached from D_{12}. Now suppose that the intersection point of $\hat{\varphi}$ with the x_2-axis is below $w^+(-\rho_m, -\rho_a)$, then it is possible to steer the system from $e_2(-\rho_a)$ to $-\infty$. By continuous dependence on the initial value, this is also possible from points in R (cp. Figure 8). This contradicts positive invariance, implying that the region R is void, i.e., $\rho_m \geq I(\rho_a)$. We have shown that $I(\rho_a)$ is given by the ρ_m-value where the intersection point of $\hat{\varphi}$ with the x_2-axis coincides with $w^+(-\rho_m, -\rho_a)$.

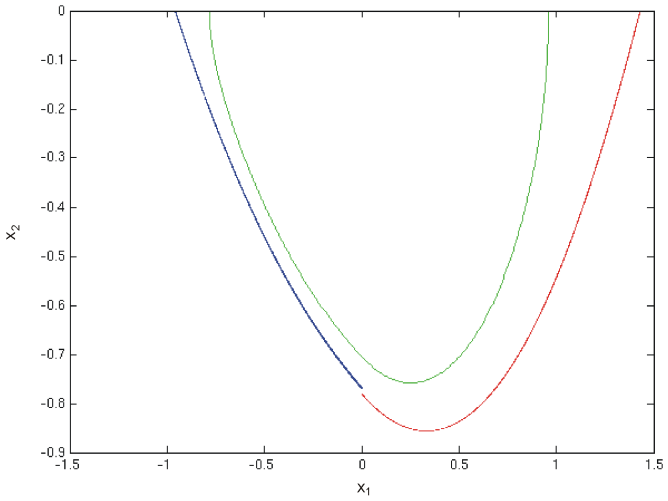

Figure 7: Stable manifold $W^+(e_1(-\rho_a), -\rho_m, -\rho_a)$ (blue), unstable manifold $W^-(e_2(-\rho_a), \rho_m, -\rho_a)$ (red) and trajectory $\hat{\varphi}(\cdot)$ (green) corresponding to control (13) for $\rho_a = 0.000$ and $\rho_m = 0.380$. Here $H(0) < \rho_m < I(0)$.

Again using monotonicity one can, by bisection, approximate the invariance margin by analyzing the relative positions of intersection points with the x_2-axis. Hence, in analogy to the heteroclinic margin, computation of

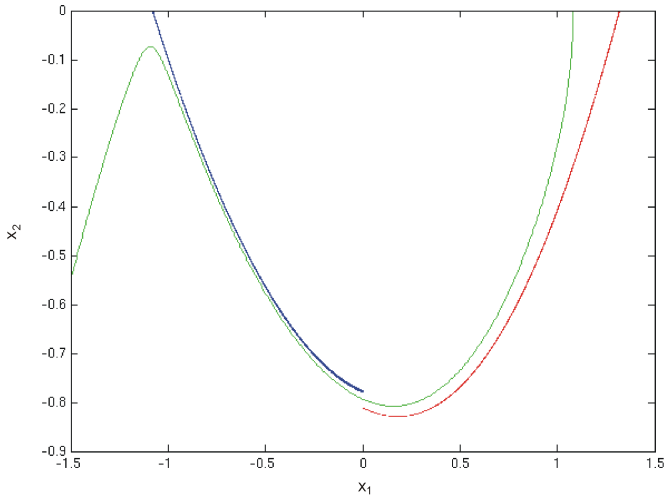

Figure 8: Stable manifold $W^+(e_1(-\rho_a), -\rho_m, -\rho_a)$ (blue), unstable manifold $W^-(e_2(-\rho_a), \rho_m, -\rho_a)$ (red) and trajectory $\hat{\varphi}(\cdot)$ (green) corresponding to control (13) for $\rho_a = 0.230$ and $\rho_m = 0.000$. Here $\rho_a > I^{-1}(0)$.

the stable manifold $W^+(e_1(-\rho_a), -\rho_m, -\rho_a)$ and the trajectory $\hat{\varphi}$ near the x_2-axis yields the following inclusions for the invariance margin $I(\rho_a)$:

$$I(0) \in (0.42, 0.43), I^{-1}(0.30) \in (0.06, 0.07), I(0.11) \in (0.20, 0.21). \quad (14)$$

One finds good agreement with the results (5) based on control set numerics. However, for $\rho_m = 0$ a slightly higher interval is obtained:

$$I^{-1}(0) \in (0.22, 0.23). \quad (15)$$

4 Melnikov Analysis and Comparison

In this section, we apply Melnikov's method to the system with M–potential (10) and compare the results to those from the control set analysis in the preceding section. We freely use results for Melnikov's method originally developed on the basis of a two-dimensional Poincaré map of a periodically forced planar system (for a detailed discussion see [9] and [15]). An extension to a sequence of maps for quasi-periodically forced systems of the type (3) was given by Beigie, Leonard, and Wiggins [1]. In the limiting case (as the number of frequency components tends to infinity) a generalized Melnikov function can be defined for an arbitrary time-dependent excitation [12].

Setting $\varepsilon = 0$ in system (10) we obtain the Hamiltonian equation

$$\dot{x}_1 = x_2,\ \dot{x}_2 = -x_1 + \alpha x_1^3.$$

The equilibria are the origin (a center) and the hyperbolic equilibria $e_1(0)$ and $e_2(0)$. Furthermore, one finds two heteroclinic orbits connecting $e_1(0)$ and $e_2(0)$ and vice versa given explicitly (cp. [12, Section 6.1]) by

$$x_{1h}(t) = \pm\frac{1}{\sqrt{\alpha}}\tanh\frac{t}{\sqrt{2}} \quad \text{and} \quad x_{2h}(t) = \pm\frac{1}{\sqrt{2\alpha}}\operatorname{sech}^2\frac{t}{\sqrt{2}}$$

with $-\infty < t < \infty$.

For $\varepsilon > 0$ the Melnikov function $M(t_0)$ measures the distance between the stable and the unstable manifold in a two-dimensional cross section in phase space at time t_0

$$\begin{aligned} M(t_0) = &-\int_{-\infty}^{\infty}\left[\beta_1 x_{2h}^2(t) + \beta_3 x_{2h}^4(t)\right]\,\mathrm{d}t \\ &+\int_{-\infty}^{\infty}\left[\rho_a u_a(t+t_0)x_{2h}(t) - \rho_m u_m(t+t_0)x_{1h}(t)x_{2h}(t)\right]\,\mathrm{d}t. \end{aligned}$$

If the Melnikov function has simple zeros, the stable and the unstable manifolds intersect transversally for small $\varepsilon > 0$.

Considering the harmonic control functions

$$u_a(t) = \rho_a\cos(\omega_a t + \psi_a), \quad u_m(t) = \rho_m\cos(\omega_m t + \psi_m), \tag{16}$$

the Melnikov function yields

$$\begin{aligned} M(t_0) = &-\beta_1\frac{2\sqrt{2}}{3\alpha} - \beta_3\frac{8\sqrt{2}}{35\alpha^2} \\ &+\rho_a\frac{\sqrt{2}\pi\omega_a\cos(\omega_a t_0 + \psi_a)}{\sqrt{\alpha}\sinh\frac{\sqrt{2}\pi\omega_a}{2}} - \rho_m\frac{\pi\omega_m^2\sin(\omega_m t_0 + \psi_m)}{\alpha\sinh\frac{\sqrt{2}\pi\omega_m}{2}}. \end{aligned}$$

For given frequencies ω_a, ω_m and phases ψ_a, ψ_m one may find amplitudes ρ_a, ρ_m such that $M(t_0) = 0$, i.e. that transverse intersections occur.

Concerning the relation between the control set analysis and Melnikov's method, we have the following results.

Theorem 4.1 *Suppose that the Melnikov function for the periodic control functions (16) with amplitudes ρ_a and ρ_m, respectively, has a simple zero at $\varepsilon = 0$. Then for all $\varepsilon > 0$, small enough, there exists a heteroclinic control set D_{12}^{ε} containing both sets of hyperbolic equilibria for system (10).*

Proof. Fix $\varepsilon > 0$, small enough. The equilibrium $e_2^\varepsilon(0,0)$ of the system with $\rho_a = \rho_m = 0$ is in the interior of a control set D_2^ε. The period map for (16) has a hyperbolic fixed point $f_2^\varepsilon(\rho_a, \rho_m)$ and it is in the interior of a control set. Also for all $\sigma_a \in [0, \rho_a)$ and $\sigma_m \in [0, \rho_m)$ the hyperbolic fixed points $f_2^\varepsilon(\sigma_a, \sigma_m)$ corresponding to the periodic controls

$$u_a(t) = \sigma_a \cos(\omega_a t + \psi_a),\ u_m(t) = \sigma_m \cos(\omega_m t + \psi_m)$$

are in the interior of some control sets. Since these fixed points change continuously with σ_a and σ_m and $f_2^\varepsilon(0,0) = e_2^\varepsilon(0,0)$, all these points are in the interior of the same control set. The same arguments apply to the hyperbolic fixed points $f_1^\varepsilon(\sigma_a, \sigma_m)$ on the left side.

Since the Melnikov function depends continuously differentiable on the amplitudes σ_a and σ_m of the periodic controls, it also has a simple zero for amplitudes less than ρ_a and ρ_m. Thus, in the lower halfplane, one finds, arbitrarily close to the hyperbolic fixed points $f_2^\varepsilon(\sigma_a, \sigma_m)$ and $f_1^\varepsilon(\sigma_a, \sigma_m)$, points on the unstable and on the stable manifolds. Hence it is possible to steer the system from the control set around the right set of equilibria to the control around the left set of equilibria. Similarly, one can steer the system in the upper halfplane in the other direction. This proves that the heteroclinic control D_{12}^ε containing both sets of hyperbolic equilibria exists. ■

A consequence of this theorem is that Melnikov's method will predict a positive capsize probability for all

$$\rho_m > \inf_{\varepsilon > 0} H^\varepsilon(\rho_a),$$

where $H^\varepsilon(\rho_a)$ is the heteroclinic margin for system (10).

Next we compare the results above with those obtained from the control set analysis in Section 3. Replacing the harmonic functions by

$$u_a(t) = \rho_a, \quad u_m(t) = -\rho_m \operatorname{sgn} t,$$

the Melnikov function yields

$$M(t_0) = -\frac{2\sqrt{2}\beta_1}{3\alpha} - \frac{8\sqrt{2}\beta_3}{35\alpha^2} + \frac{2\rho_a}{\sqrt{\alpha}} + \frac{\rho_m}{\alpha}\operatorname{sech}^2 \frac{t_0}{\sqrt{2}}.$$

Obviously, the Melnikov function has simple zeros for

$$\rho_m > \frac{2\sqrt{2}\beta_1}{3} + \frac{8\sqrt{2}\beta_3}{35\alpha} - 2\sqrt{\alpha}\rho_a.$$

For the parameter values $\alpha = 0.674$, $\beta_1 = 0.231$, and $\beta_3 = 0.375$, we obtain

$$\rho_m > 0.3976 - 1.6420\rho_a.$$

These results are compared to the numerical computation for $\varepsilon = 1, \frac{1}{2}, \frac{1}{4}$, see Table 1. Apparently, the heteroclinic margin for $\varepsilon \to 0$ approaches the critical value predicted by Melnikov's method.

Table 1: Comparison of the heteroclinic margin and the results of Melnikov's method for $\varepsilon = 1, \frac{1}{2}, \frac{1}{4}$.

Case	$H(\rho_a = 0)$	$H^{-1}(\rho_m = 0)$
$\epsilon = 1$	$0.370 \ldots 0.380$	$0.220 \ldots 0.230$
$\epsilon = \frac{1}{2}$	$0.385 \ldots 0.395$	$0.230 \ldots 0.240$
$\epsilon = \frac{1}{4}$	$0.390 \ldots 0.400$	$0.235 \ldots 0.245$
Melnikov	0.398	0.242

5 The Perturbed Escape Equation

In this section we discuss the perturbed escape equation and again compare results from Melnikov's method with results based on control set analysis; for the latter, we rely in particular on the paper by Gayer [8].

Consider the perturbed escape equation

$$\dot{x}_1 = x_2,\ \dot{x}_2 = -\varepsilon\gamma\, x_2 - x_1 + {x_1}^2 + \varepsilon F\, \sin\omega t + \varepsilon u_a(t)$$

with $u(t) \in [-\rho_a, \rho_a]$ and parameter values

$$\gamma = 0.1,\ \omega = 0.85,\ F = 0.06. \tag{17}$$

The corresponding Hamiltonian system ($\varepsilon = 0$, see Figure 9) has an equilibrium at the origin (a center) and a hyperbolic equilibrium $e^0 = (1, 0)$ with a homoclinic orbit given by

$$x_{1h}(t) = \frac{3}{2}\tanh^2\frac{t}{2} - \frac{1}{2}, \quad x_{2h}(t) = \frac{3}{2}\mathrm{sech}^2\frac{t}{2}\tanh\frac{t}{2}. \tag{18}$$

For the perturbation $u_a(t) = \rho_a \mathrm{sgn}\, t$, we obtain the Melnikov function

$$M(t_0) = -\frac{6\gamma}{5} + \frac{6F\pi\omega^2\cos\omega t_0}{\sinh\pi\omega} + 3\rho_a\mathrm{sech}^2\frac{t_0}{2}.$$

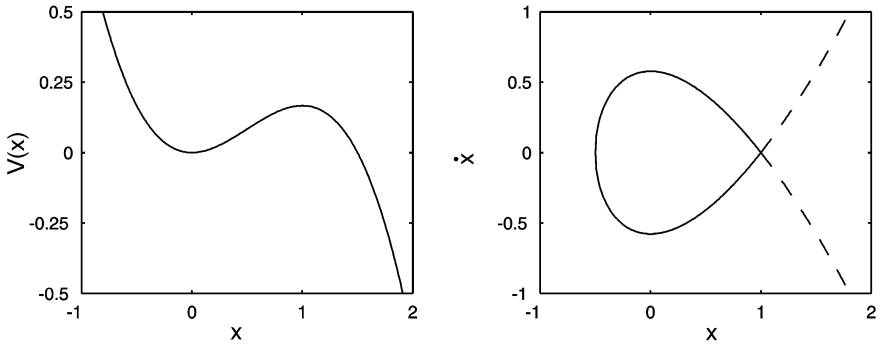

Figure 9: Potential (left) and corresponding homoclinic orbit (right) of the escape equation.

Thus, transverse intersections occur first close to $t_0 = 0$ if

$$\rho_a > \frac{2\gamma}{5} - \frac{2F\pi\omega^2}{\sinh \pi\omega}.$$

In the absence of periodic forcing (i.e., $F = 0$), the critical control amplitude is

$$\rho_a = 0.04.$$

This value coincides with the numerical calculations in [7] (for $\varepsilon = 1$). For the parameters (17) the critical control amplitude is

$$\rho_a = 0.0021. \tag{19}$$

On the other hand, the numerical control set analysis performed in Gayer [8] for the case $\varepsilon = 1$ shows the following, more elaborate pattern when the amplitude ρ_a is increased:

First we recall that the uncontrolled system suffers a bifurcation when F is increased from zero. For the parameters (17) there are two orbitally stable periodic solutions and two hyperbolic periodic solutions. Then, for small amplitude $\rho_a = 0.005$, they are included in the interior of control sets D_1, D_2, D_3, D_4. Here D_1 and D_3 are invariant control sets, while D_2 (in the potential well) and D_4 (on the potential hill top) are variant control sets. For $\rho_a = 0.0085$, the two control sets D_1 and D_2 have merged into a variant control set D_{12}, while D_3 and D_4 remain distinct. For $\rho_a = 0.01$ also the control sets D_{12} and the invariant control set D_3 have merged into an invariant control set D_{123} and, finally, for $\rho_a = 0.013$ also the control set

D_4 has merged with D_{123} forming a variant control set D_{1234}. In this latter situation, no invariance properties prevail. Hence Gayer's numerical results in [8] show that the invariance margin $I_{inv}(\rho_a)$ satisfies

$$0.01 < I_{inv}^{-1}(0) < 0.013.$$

This is an enclosure for the critical amplitude where loss of invariance occurs, since for $\rho_a \leq 0.01$ all points in the invariant control set D_{123} containing the origin remain in this set with probability one; for $\rho_a \geq 0.013$ the control set D_{1234} around the origin has lost its invariance and for every x in this control set the expectation of the sojourn time is finite.

As a consequence of the Melnikov result, we see that, due to the transversal intersections of the stable and unstable manifolds of the hyperbolic fixed point $f^\varepsilon(\rho_a)$, there exists a homoclinic control set D_{44}^ε for small $\varepsilon > 0$ provided that ρ_a is greater than the critical amplitude (19). In its interior it contains the (chaotic) invariant set of a $k-$fold concatenation of the period map as predicted by Melnikov; furthermore it contains the hyperbolic fixed point $f_4^\varepsilon(0)$. Thus the set of complete controllability D_4^ε containing the periodic solution on the hill top is a proper subset of D_{44}^ε and hence D_4^ε is not a control set, but just a local control, i.e., a subset of complete controllability which is maximal only in a neighborhood. Note, however, that analytically, it is not clear if the control set D_{44}^ε also exists for $\varepsilon = 1$ (this is the situation discussed in [8]).

6 Conclusions

The analysis of two models for ship roll motion and capsizing illustrates that Melnikov's method does not indicate the loss of integrity; instead it is related to the existence of heteroclinic connections and hence to the heteroclinic margin which is strictly less than the invariance margin. The same appears to hold as well for perturbations of Hamiltonian systems with homoclinic orbits. Furthermore, in its range of validity Melnikov's methods gives very accurate predictions for the homoclinic or heteroclinic margin.

For a dominant sinusoidal (in the escape equation), the value predicted by the Melnikov method is far below numerical results for the invariance margin. Hence it appears to be far too conservative. Certainly, the situation of perturbations with dominant sinusoidal components needs further analysis.

Acknowledgement. The numerical computation of the control sets are due to Johannes Taubert and Dirk Wohlgemuth.

References

[1] D. Beigie, A. Leonard, and S. Wiggins, *Chaotic transport in the homoclinic and heteroclinic tangle regions of quasiperiodically forced two-dimensional dynamical systems*, Nonlinearity, 41 (1991), pp. 775–819.

[2] F. Colonius, F. J. de la Rubia, and W. Kliemann, *Stochastic models with multistability and extinction levels*, SIAM J. Appl. Math., 56 (1996), pp. 919–945.

[3] F. Colonius, T. Gayer, and W. Kliemann, *Near invariance for Markov diffusion systems*. submitted, 2004.

[4] F. Colonius and W. Kliemann, *Continuous, smooth, and control techniques for stochastic dynamics*, in Stochastic Dynamics, H. Crauel and M. Gundlach, eds., Springer-Verlag, 1999, pp. 181–208.

[5] ——, *The Dynamics of Control*, Birkhäuser, 2000.

[6] M. Dellnitz and A. Hohmann, *A subdivision algorithm for the computation of unstable manifolds and global attractors*, Numerische Mathematik, 75 (1997), pp. 293–317.

[7] T. Gayer, *Controlled and perturbed systems under papameter variation*, 2003, Dissertation, Universität Augsburg, Augsburg, Germay.

[8] ——, *Controllability and invariance properties of time-periodic systems*, Int. J. Bifurcation and Chaos, 15 no.4 (2005), pp. 1361–1375.

[9] J. Guckenheimer and P. Holmes, *Nonlinear Oscillations, Dynamical Systems and Bifurcation of Vector Fields*, Springer-Verlag, Berlin, 1986.

[10] E. Kreuzer and W. Sichermann, *Investigation of large amplitude roll motions and capsizing*, in Proceedings of the Ninth International Symposium on Practical Design of Ships and Other Floating Structures, H. Keil and E. Lehmann, eds., Hansa Verlag, 2004, pp. 689–696.

[11] H. Nusse, E. Ott, and J. Yorke, *Saddle-node bifurcations on fractal boundaries*, Phys. Rev. Lett., 75 (13) (1995), pp. 2482–2485.

[12] E. Simiu, *Chaotic Transitions in Deterministic and Stochastic Systems*, Princeton University Press, 2002.

[13] M. Soliman and J. Thompson, *Basin organization prior to a tangled saddle-node bifurcation*, Int. J. Bifurcation and Chaos, 1 (1991), pp. 107–118.

[14] D. Szolnoki, *Set oriented methods for computing reachable sets and control sets*, Discrete and Continuous Dynamical Systems-Series B, 3 (2003), pp. 361–382.

[15] S. Wiggins, *Global Bifurcations and Chaos. Analytical Methods*, Springer-Verlag, 1988.